
SODA10M: Towards Large-Scale Object Detection Benchmark for Autonomous Driving

Jianhua Han^{1*} Xiwen Liang^{2*} Hang Xu^{1†} Kai Chen³ Lanqing Hong¹
Chaoqiang Ye¹ Wei Zhang¹ Zhenguo Li¹ Xiaodan Liang^{2†} Chunjing Xu¹

Abstract

Aiming at facilitating a real-world, ever-evolving and scalable autonomous driving system, we present a large-scale benchmark for standardizing the evaluation of different self-supervised and semi-supervised approaches by learning from raw data, which is the first and largest benchmark to date. Existing autonomous driving systems heavily rely on ‘perfect’ visual perception models (e.g., detection) trained using extensive annotated data to ensure the safety. However, it is unrealistic to elaborately label instances of all scenarios and circumstances (e.g., night, extreme weather, cities) when deploying a robust autonomous driving system. Motivated by recent powerful advances of self-supervised and semi-supervised learning, a promising direction is to learn a robust detection model by collaboratively exploiting large-scale unlabeled data and few labeled data. Existing dataset (e.g., KITTI, Waymo) either provides only a small amount of data or covers limited domains with full annotation, hindering the exploration of large-scale pre-trained models. Here, we release a Large-Scale Object Detection benchmark for Autonomous driving, named as **SODA10M**, containing 10 million unlabeled images and 20K images labeled with 6 representative object categories. To improve diversity, the images are collected every ten seconds per frame within 32 different cities under different weather conditions, periods and location scenes. We provide extensive experiments and deep analyses of existing supervised state-of-the-art detection models, popular self-supervised and semi-supervised approaches, and some insights about how to develop future models. We show that SODA10M can serve as a promising pre-training dataset for different self-supervised learning methods, which gives superior performance when finetuning autonomous driving downstream tasks. This benchmark will be used to hold the ICCV2021 SSLAD challenge. The data and more up-to-date information have been released at <https://soda-2d.github.io>.

1 Introduction

Autonomous driving technology has been significantly accelerated in recent years because of its great potential in reducing accidents, saving human lives and improving efficiency. As an essential module in the visual perception system, object detection in road images plays one of the most critical roles for autonomous driving.

Performances of current object detection approaches, however, may be limited by the currently available datasets [7, 64, 49], due to the drawbacks of existing benchmarks. First, the diversity of data sources is lacking. For example, the largest self-driving dataset in existence, Waymo Open [49], was

¹ Huawei Noah’s Ark Lab

² Sun Yat-Sen University

³ Hong Kong University of Science and Technology * These two authors contribute equally.

[†] Corresponding authors: xdliang328@gmail.com & xu.hang@huawei.com

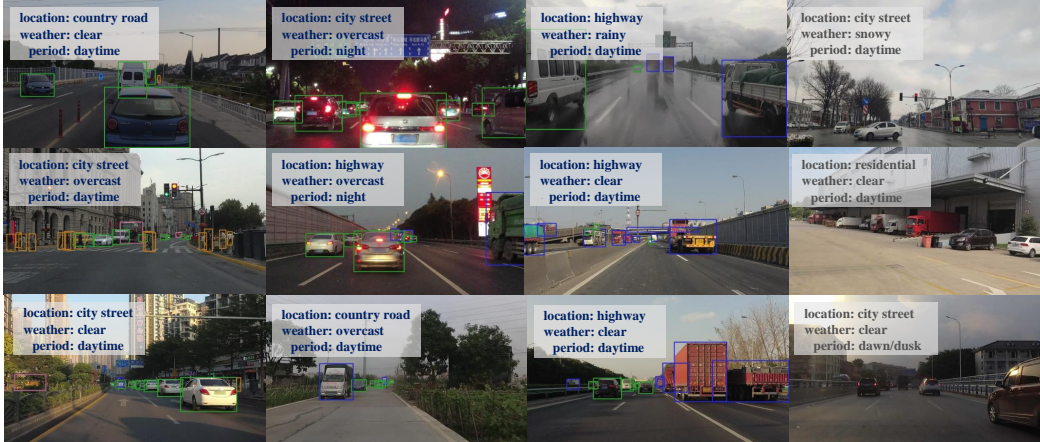


Figure 1: Examples of challenging environments in our dataset. The first three columns of images are from SODA10M labeled set, and the last column is from the unlabeled set. Our dataset includes a diverse set of 10 million images under different weather conditions, periods and locations.

collected from only three cities, covering only a few scenarios and circumstances. Models trained on these datasets may overfit to specific scenarios or characteristics. Second, existing datasets are usually fully annotated but limited in scale due to the cost of data annotation. They are not able to support the exploration of autonomous driving with huge volumes of unlabeled data.

Numerous self-supervised techniques [4, 19, 21, 5] have been developed for vision tasks to solve this problem, showing competitive or even superior performance compared with supervised learning. The main idea is to learn representation from a large set of unlabeled images via pretext tasks rather than annotation. Research efforts have also been devoted to semi-supervised learning [44, 41, 65, 31], such as self training and consistency regularization, which collaboratively exploits both labeled data and large-scale unlabeled data to boost performance. Existing self-supervised and semi-supervised methods are mainly evaluated on ImageNet[8] and MSCOCO[37], where data labels are artificially removed for demonstration. There is no available benchmark for investigating advanced self-supervised and semi-supervised techniques for autonomous driving with real large-scale data.

To boost the development of real-world autonomous driving systems, we develop the first and largest-Scale **O**bject **D**etection benchmark for **A**utonomous driving (SODA10M) that contains 10 million road images. Our SODA10M dataset can be distinguished from existing datasets from three aspects, including *scale*, *diversity* and *generalization*.

Scale. As shown in Table 1, SODA10M is significantly larger than existing autonomous driving datasets like BDD100K [64] and Waymo [49]. It contains 10 million images of road scenes, which is ten times more than Waymo [49]. Specifically, 20K images with tightly fitting high-quality 2D bounding boxes while 10M images are unlabeled. All images contain detailed geographical, chronological and weather information.

Diversity. As shown in Fig. 1, SODA10M comprises images covering four seasons in 32 cities under different scenarios (e.g., urban, rural) and circumstances (e.g., night, rain, snow), while most present self-driving datasets [67, 64, 49] are less diverse. The changing scenarios and circumstances result in significant domain gaps in SODA10M. Specifically, the labeled training set contains only one domain, while the validation set and the unlabeled set contain 18 and 48 domains, respectively, which can serve as a challenging benchmark for unsupervised or semi-supervised domain adaptation.

Generalization. The largest scale and diversity ensure SODA10M’s superior generalization ability as a pre-training dataset over all existing autonomous-driving datasets. Observed from evaluations of existing self-supervised algorithms, the representations learned from SODA10M unlabeled set are superior to that learned from other driving datasets like Waymo [49], i.e., 38.9% vs. 37.1% in mAP for object detection task on SODA10M labeled set and 75.2% vs. 73.8% for semantic segmentation task on Cityscapes [7] when using MoCov1 [21] (see Sec. 4.3 for more details).

Table 1: Comparison of dataset statistics with existing popular benchmarks. Night/Rain indicates whether the dataset has domain information related to night or rainy scenes. Video represents whether the dataset provides video format or detailed chronological information.

Dataset	Images	Cities	Night/Rain	Video	Categories	Boxes	Resolution
Caltech Pedestrian [10]	249K	5	X/X	✓	1	347K	640×480
KITTI [14]	15K	1	X/X	X	3	80K	1382×512
Citypersons [67]	5K	27	X/X	X	1	35K	2048×1024
BDD100K [64]	100K	4	✓/✓	✓	10	4.2M	1280×720
Waymo Open [49]	1M	3	✓/X	✓	3	9.9M	1920×1280
SODA10M (Ours)	10M	32	✓/✓	✓	6	149K	1920×1080

We provide experiments and in-depth analysis of existing supervised detection models, prevailing self-supervised and semi-supervised approaches on SODA10M. Observation can be made that simple self-supervised methods (e.g., MoCo-v1 [21]) achieve better results than the dense contrastive ones (e.g., DenseCL [56]) on SODA10M unlabeled set and semi-supervised methods work much better than self-supervised methods, even with a smaller set of unlabeled data (1-million vs. 5-million).

This benchmark will be used to hold the ICCV2021 SSLAD challenge, which aims to investigate current ways of building next-generation industry-level autonomous driving systems by resorting to self-supervised and semi-supervised learning. The SODA10M dataset and more up-to-date related information have been released and will be maintained weekly.

2 Related Work

Driving datasets have gained enormous attention due to the popularity of autonomous self-driving. Several datasets focus on detecting specific objects such as pedestrians [10, 67]. Cityscapes [7] provides instance segmentation on sampled frames, while BDD100K [64] is a diverse dataset under various weather conditions, time and scene types for multitask learning. For 3D tasks, KITTI Dataset [15, 14] was collected with multiple sensors, enabling 3D tasks such as 3D object detection and tracking. Waymo Open Dataset [49] provides large-scale annotated data with 2D and 3D bounding boxes, and nuScenes Dataset [1] provides rasterized maps of relevant areas.

Supervised learning methods for object detection can be roughly divided into single-stage and two-stage models. One-stage methods [36, 12, 38] directly outputs probabilities and bounding box coordinates for each coordinate in feature maps. On the other hand, two-stage methods [22, 45, 35] use a Region Proposal Network (RPN) to generate regions of interests, then each proposal is sent to obtain classification score and bounding-box regression offsets. By adding a sequence of heads trained with increasing IoU thresholds, Cascade RCNN [2] significantly improves detection performance. With the popularity of the vision transformer, more and more transformer-based object detectors [55, 40] have been proposed.

Self-supervised learning approaches can be mainly divided into pretext tasks [9, 66, 43, 42] and contrastive learning [21, 5, 4, 19]. Pretext tasks often adopt reconstruction-based loss functions [9, 43, 17] to learn visual representation, while contrastive learning is supposed to pull apart negative pairs and minimize distances between positive pairs, achieved by training objectives such as InfoNCE [53]. MoCo [21, 5] constructs a queue with a large number of negative samples and a moving-averaged encoder, while SimCLR [4] explores the composition of augmentations and the effectiveness of non-linear MLP heads. SwAV [3] introduces cluster assignment and swapped prediction to be more robust about false negatives, and BYOL [19] demonstrates that negative samples are not prerequisite to learn meaningful visual representation. For video representation learning, early methods are based on input reconstruction [24, 25, 32, 33], while others define different pretext tasks to perform self-supervision, such as frame order prediction [34], future prediction [48, 54] and spatial-temporal jigsaw [30]. More recently, contrastive learning is integrated to learn temporal changes [18, 63].

Semi-supervised learning methods mainly consist of self training [61, 59] and consistency regularization [46, 65, 20]. Consistency regularization tries to guide models to generate consistent predictions between original and augmented inputs. In the field of object detection, previous works focus on training detectors with a combination of labeled, weakly-labeled or unlabeled data [26, 50, 13], while recent works [28, 47] train detectors with a small set of labeled data and a larger amount of unlabeled images. Specifically, STAC [47] pre-trains the object detector with labeled data and generate pseudo labels on unlabeled data, which are used to finetune the pre-trained model. Unbiased Teacher [39] further improves the process of generating pseudo labels via teacher-student mutual learning.

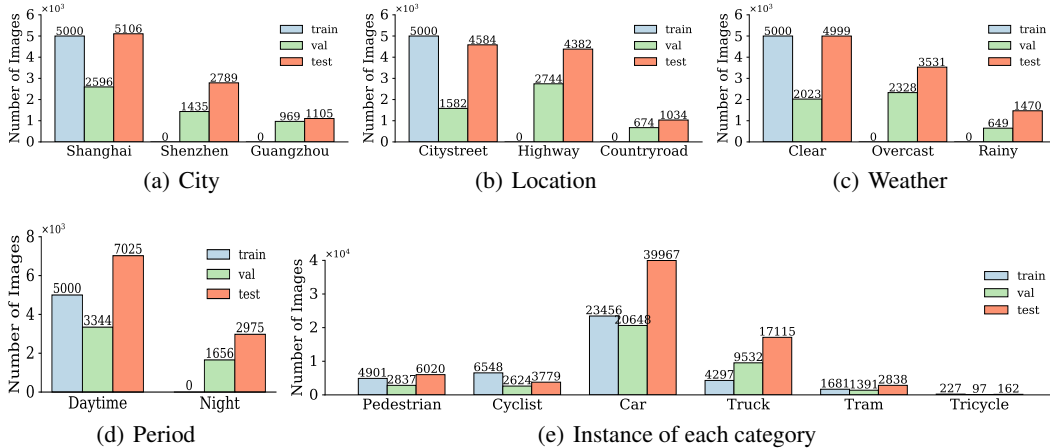


Figure 2: Statistics of the labeled set. (a) Number of images in each city. (b) Number of images in each location. (c) Number of images in each weather condition. (d) Number of images in each period. (e) Number of instances in each category.

3 SODA10M

We collect and release a large-scale 2D dataset to promote significant progress of self-supervised and semi-supervised learning in autonomous driving. Our SODA10M contains 10M unlabeled images and 20K labeled images, which is split into training(5K), validation(5K) and testing(10K) sets.

3.1 Data Collection

The image collection task is distributed to the tens of thousands of taxi drivers in crowdsourcing. They have to use the mobile phone or driving recorder (1080P+) to obtain images every ten seconds per frame. Horizon needs to be kept at the center of the image, and the occlusion inside the car should not exceed 15% of the whole picture. Images should be obtained in diverse weather conditions, periods, locations and cities to achieve more diversity. After receiving each batch of images from the suppliers, a random 5% of pictures will be selected for manual verification. Batches of images with a pass rate below 95% will be returned for rectification.

Data Protection The driving scenes are collected in permitted areas. We comply with the local regulations and avoid releasing any localization information, including GPS and cartographic information. For privacy protection, we actively detect any object on each image that may contain personal information, such as human faces and license plates, with a high recall rate. Then, we blur those detected objects to ensure that no personal information is disclosed. Detailed licenses, terms of use and privacy are listed in Appendix A.

3.2 Annotation

Image tags (i.e., weather conditions, location scenes, periods) for all images and 2D bounding boxes for labeled parts should be annotated for SODA10M. To ensure high quality and efficiency, the whole annotation progress can be divided into the following three different steps.

Pre-annotation: In order to ensure efficiency, a multi-task detection model, which is based on Faster RCNN [45] and searched backbone [29, 62], is trained on millions of Human-Vehicle images with bounding-box annotation and generate coarse labels for each image first.

Annotation: Based on pre-annotated labels, annotators keep the accurate ones and correct the inaccurate labels. Each image is distributed to different annotators, and the images with the same annotation will be passed to the following process; otherwise, they would be distributed again. All annotators must participate in several courses and pass the examination for standard labeling.

Examination: Senior annotators with rich annotation experience will review the image annotations in the second step, and the missing or incorrectly labeled images will be sent back for re-labeling.

We exhaustively annotated car, truck, pedestrian, tram, cyclist and tricycle with tightly-fitting 2D bounding boxes in 20K images. The bounding-box label is encoded as (x, y, w, h) , where x and y represent the top-left pixel of the box, and w and h represent the width and length of the box.

3.3 Statistics

Labeled Set. The labeled set contains 20K images with full annotation. There are 5K images for training, 5K images for validation and 10K images for testing. As shown in Fig. 2, the training set only contains images obtained in city streets of Shanghai with clear weather in the daytime, while the validation and testing sets have three weather conditions, locations, cities and two different periods of the day. Considering the small gap between domains in different cities, we define 18 fine-grained domains through the pairwise combination of the remaining domains. The number of images in each fine-grained domain in the validation set and testing set are shown in Appendix D.

Unlabeled Set. The unlabeled set contains 10M images with diverse attributes. As shown in Fig. 3(a), the unlabeled images are collected among 32 cities, covering a large part of eastern China. Compared with the labeled set, the unlabeled set contains not only many more cities but also additional scenes such as residential, snowy and dawn/dusk, according to the gray part in Fig. 3(b), Fig. 3(c) and Fig. 3(d). The rich diversity in SODA10M unlabeled set ensures the generalization ability to transfer to other downstream autonomous driving tasks as a pre-training or self-training dataset.

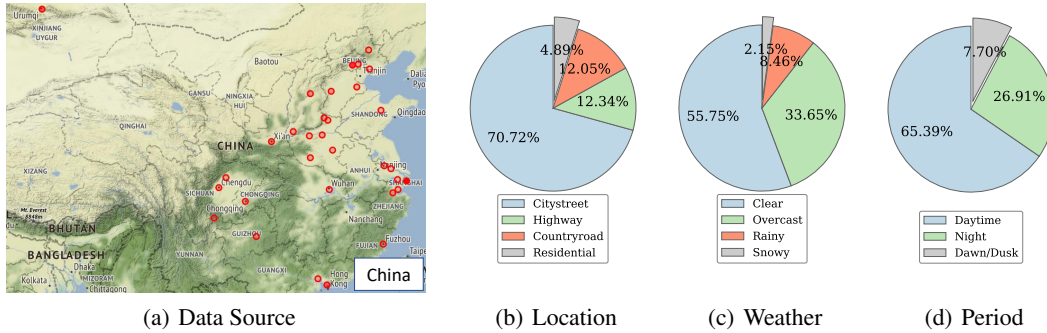


Figure 3: Statistics of the unlabeled set. (a) Geographical distribution of our data sources. SODA10M is collected from 32 cities, and darker color indicates greater quantity. (b) Number of images in each location. (c) Number of images in each weather condition. (d) Number of images in each period.

4 Benchmark

As SODA10M is regarded as a new autonomous driving benchmark, we provide the fully supervised baseline results based on several representative one-stage and two-stage detectors. With the massive amount of unlabeled data, we then study the generalization ability of state-of-the-art self-supervised and semi-supervised methods based on SODA10M and give insights into developing future models. Methods used for building this benchmark are representative samples of Fig. 4. To make the experiments easily reproducible, the code of all used methods has been open-sourced, and detailed experiment settings and training time comparisons are provided in Appendix B.

4.1 Basic Settings

We utilize Detectron2 [57] as our codebase for the following experiments. Following the default settings in Detectron2, we train detectors with 8 Tesla V100 with a batch size 16. For the 1x schedule, the learning rate is set to 0.02, decreased by a factor of 10 at 8th, 11th epoch of total 12 epochs, while 2x indicates 24 epochs. Multi-scale training and SyncBN are adopted in the training process and precise-BN is used during the testing process. The image size in the testing process is set to 1920×1080 . Unless specified, the algorithms are tested on the validation set of SODA10M. COCO API [37] is adopted to evaluate the detection performance for all categories.

4.2 Supervised Learning Benchmark

As shown in Table 2, the detection results of four popular object detectors (RetinaNet [36], Faster RCNN [45], Cascade RCNN [2]) are compared. We observe that in the 1x schedule, Faster RCNN exceeds RetinaNet in mAP by 5.3% with a larger number of parameters, which is consistent with the traditional difference of single-stage and two-stage detectors. Equipped with a stronger head, Cascaded RCNN can further surpass Faster RCNN by a large margin (3.9%). Observation can also be made that training with a longer schedule can further improve the performance.

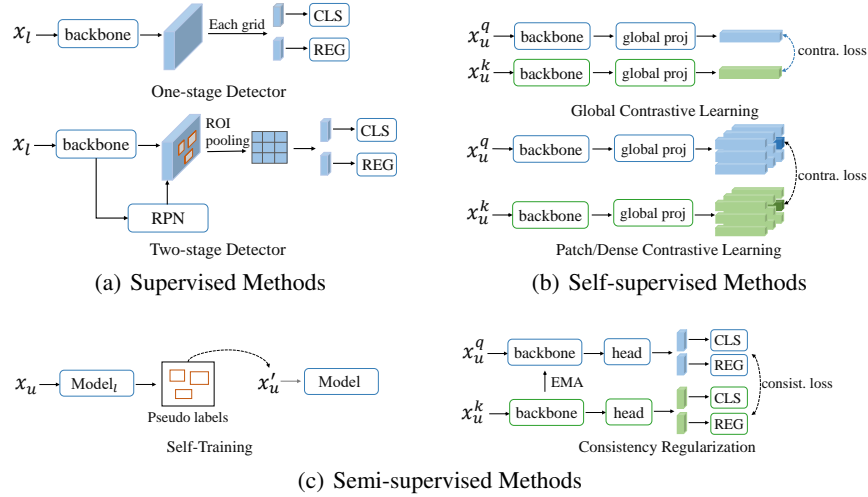


Figure 4: Overview of different methods used for building SODA10M benchmark. X_l and X_u denote for labeled set and unlabeled set. q, k represent for different data augmentations. For semi-supervised learning methods, the labeled set is also involved in training progress with supervised loss.

Table 2: Detection results(%) of baseline models on SODA10M dataset.

Model	Split	mAP	Pedrian	Cyclist	Car	Truck	Tram	Tricycle	Params
RetinaNet [36] 1x	Val	32.7	23.9	37.3	55.7	40.0	36.6	3.0	36.4M
RetinaNet [36] 2x	Val	35.0	26.6	39.4	57.2	41.8	38.2	6.5	36.4M
RetinaNet [36] 2x	Test	34.0	24.9	36.9	57.5	44.7	32.1	7.8	36.4M
Faster RCNN [45] 1x	Val	37.9	31.0	43.2	58.3	43.2	41.3	10.5	41.4M
Faster RCNN [45] 2x	Val	38.7	32.5	43.6	58.9	43.7	40.8	12.6	41.4M
Faster RCNN [45] 2x	Test	36.7	29.5	40.1	59.7	47.2	32.3	11.7	41.4M
Cascade RCNN [2] 1x	Val	41.9	34.6	46.7	61.9	47.2	45.1	16.0	69.2M
Cascade RCNN [2] 1x	Test	39.4	31.9	43.4	62.6	50.0	36.8	11.9	69.2M

Precision recall (PR) curves (from COCO eval API [37]) of each category for Faster RCNN 1x are shown in Fig. 5. Observation can be made that for categories with a small number of instances (Tricycle, Tram and Pedestrian), the error types are mainly from many false positives (FP) with class confusion, which is shown in the green part. On the contrary, for the primary category like Car, FP has little impact on the performance. Note that each category in SODA10M is a singleton supercategory so its Sim result is identical to Loc. We also illustrate the PR curves of Cascade RCNN 1x and find that the error type is basically consistent with Faster RCNN while Cascade RCNN shows stronger detection performance.

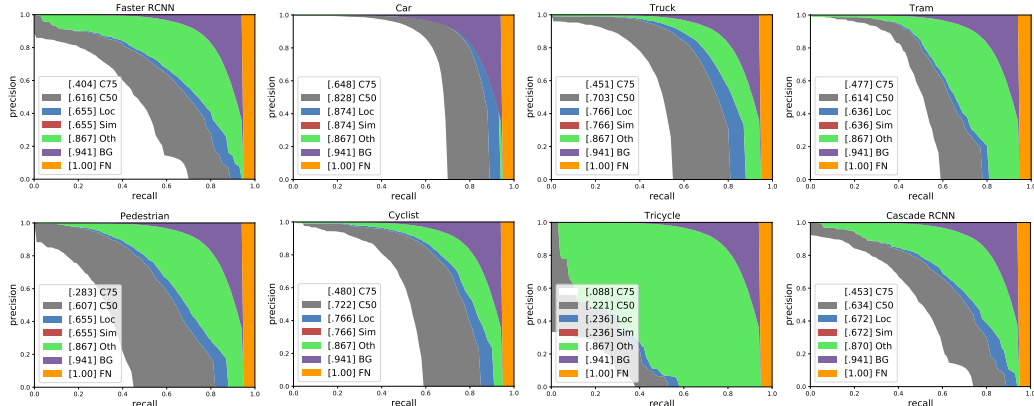


Figure 5: Precision recall curves of each category for Faster RCNN 1x and Cascaded RCNN 1x.

Table 3: Detection results(%) of self-supervised models evaluated on SODA10M labeled set, Cityscapes [7] and BDD100K [64]. mIOU-C, mIOU-B denotes for semantic segmentation performance on Cityscapes and BDD100K respectively. † represents for training with additional 5-million data. FCN-16s is a modified FCN with stride 16 used in MoCo [21]. 1x and 90k denote finetuning 12 epochs and 90k iterations, respectively.

Pre-trained Dataset	Method	Faster-RCNN 1x			RetinaNet 1x			FCN-16s 90k	
		mAP	AP50	AP75	mAP	AP50	AP75	mIOU-C	mIOU-B
	random init	23.0	40.0	23.9	11.8	20.8	12.0	65.3	50.7
	super. IN	37.9	61.6	40.4	32.7	53.9	33.9	74.6	58.8
ImageNet [8]	MoCo-v1 [21]	39.0	62.0	41.6	33.8	54.9	35.2	75.3	59.7
	MoCo-v2 [5]	39.5	62.7	42.4	35.2	56.4	36.8	75.7	60.0
	SimCLR [4]	37.0	60.0	39.4	29.0	49.0	29.3	75.0	59.2
	SwAV [3]	35.7	59.9	36.9	26.4	45.7	26.3	73.0	57.1
	DetCo [58]	38.7	61.8	41.3	33.3	54.7	34.3	76.5	61.6
	DenseCL [56]	39.9	63.2	42.6	35.7	57.3	37.2	75.6	59.3
Waymo [49]	MoCo-v1	37.1	59.8	39.3	31.2	51.8	32.3	73.8	57.0
	MoCo-v2 [5]	37.1	59.7	39.4	31.4	52.0	32.4	73.5	56.6
	DetCo [58]	36.3	59.1	38.4	29.4	49.4	29.9	74.6	58.2
SODA10M	MoCo-v1 [21]	38.9	62.1	41.2	33.4	54.4	34.6	75.2	59.3
	MoCo-v1† [21]	39.0	62.6	41.9	33.8	55.2	35.2	75.5	59.5
	MoCo-v2 [5]	38.7	61.5	41.4	33.3	54.1	34.7	74.2	58.2
	MoCo-v2† [5]	38.6	61.3	41.4	33.2	54.6	34.6	74.5	58.9
	SimCLR [4]	35.9	59.5	37.4	28.7	48.7	29.1	73.3	57.3
	SimCLR† [4]	37.1	60.9	39.8	30.5	51.3	31.2	73.5	58.8
	SwAV [3]	33.4	57.1	34.5	24.5	43.2	24.6	68.6	54.2
	DetCo [58]	37.7	60.6	40.1	32.4	54.1	33.4	74.1	59.3
	DenseCL [56]	38.1	60.8	40.5	33.6	54.8	35.0	75.2	57.4
	Video MoCo-v1 [21]	34.9	57.8	36.6	27.9	47.3	28.2	73.6	57.3
	Video MoCo-v2 [5]	34.8	57.0	36.5	28.9	48.6	29.5	74.4	56.8
Video VINCE [18]	34.9	57.7	36.9	27.6	47.1	28.0	72.6	57.4	
Video VINCE+Jigsaw [18]	35.5	58.1	37.0	28.2	48.1	28.6	74.1	56.9	

4.3 Self-Supervised Learning Benchmark

Self-supervised learning, especially contrastive learning methods, has raised attraction recently as it learns effective transferable representations via pretext tasks without semantic annotations. Traditional self-supervised algorithms [11, 42, 16] are usually pre-trained on ImageNet, while recent works [6, 51] have shown the consistency between upstream and downstream data distribution has a positive impact on the final performance. Therefore, we mainly compare the performance of existing mainstream self-supervised methods pre-trained on ImageNet and autonomous driving datasets, including SODA10M and Waymo [49].

We follow the default settings in OpenSelfSup¹ to train six state-of-the-art standard self-supervised learning methods, including MoCo-v1 [21], MoCo-v2 [5], SimCLR [4], SwAV [3], DetCo [58], DenseCL [56], and evaluate their performance by fine-tuning the pre-trained models on the SODA10M labeled data and other self-driving datasets like BDD100K [64] and Cityscapes [7] to verify the generalization ability. For video-based self-supervised learning, MoCo-v1 [21], MoCo-v2 [5] and VINCE [18] are adopted. To ensure fairness, we apply the same data augmentation with VINCE for better results. Due to the limit of hardware resources, we only use a 5-million unlabeled subset in each experiment by default, while we also make full use of the other 5-million subset in a sequential training manner, following Hu et al. [27]. Specifically, the model pre-trained on the first subset will be used as initialization to continue pre-training on the second one. We adopt 325-epoch and 60-epoch pre-training on Waymo and SODA unlabeled set for image-based methods respectively, to maintain similar GPU hours with pre-training 200 epochs on ImageNet for fair comparison. Video-based approaches are trained for 800 epochs by considering time limit.

ResNet-based Methods. We pre-train on three different datasets (ImageNet, Waymo and SODA10M unlabeled set), and then report the transfer performance on three downstream tasks (detection on SODA10M labeled set, semantic segmentation on Cityscapes and BDD100K) in Table 3. For different downstream detection tasks listed in this table, the MoCo methods (MoCo-v1 [21], MoCo-v2 [5]) and dense contrastive methods (DenseCL [56], DetCo [58]) can achieve better results, while the other methods perform even worse than ImageNet fully supervised pre-train. We also observe dense

¹<https://github.com/open-mmlab/OpenSelfSup>

Table 4: Detection results(%) of self-supervised models evaluated on SODA10M labeled set, Cityscapes (C) and BDD100K (B) with Transformer model (PVT). All models are pre-trained on SODA10M unlabeled set.

Model	PVT-small [55] 1x			PVT-small [55] 2x			PVT-small [55] 1x		PVT-small [55] 90k	
	mAP	AP50	AP75	mAP	AP50	AP75	mAP-C	AP50-C	mIOU-C	mIOU-B
random init	20.6	37.9	20.1	22.5	40.3	22.2	29.8	54.9	52.5	35.4
super. IN	33.8	57.3	35.2	33.0	55.1	33.9	33.8	60.0	60.0	41.8
MoCo-v1 [21]	28.7	50.3	29.1	28.5	49.7	29.1	30.4	56.4	59.2	40.3
MoCo-v2 [5]	26.2	46.8	26.3	26.7	46.5	27.4	28.3	52.5	58.1	39.4
BYOL [19]	27.4	49.2	26.9	26.9	47.4	27.1	28.0	53.1	57.6	40.5
SimCLR [4]	30.2	54.1	29.7	30.4	53.3	30.7	30.8	56.6	58.5	40.9

contrastive methods show excellent results when pre-trained on ImageNet, but relatively poor on SODA10M unlabeled set. Experiments show that the model pre-trained on ImageNet performs equivalent or better than the one in SODA10M, which is because the existing self-supervised methods are often designed for simple scenes like ImageNet and fail to deal with the complex driving scene. By comparing the results of the same self-supervised algorithm on Waymo [49], we verify that the diversity of SODA10M data can bring better generalization ability. Besides, more pre-training iterations will bring better performance. The above results inspire us to design suitable self-supervised tasks or different pre-training strategies according to complex driving scenarios. At the same time, the diversity of SODA10M unlabeled set can also ensure that SODA10M is a superior upstream pre-training dataset. More downstream tasks and comparisons on the 2x schedule are illustrated in Appendix C.

Video-based Methods. Since our unlabeled set has detailed timing information for videos, we also transform the unlabeled set into video frames whose interval is 10 seconds and perform contrastive learning on these sequential frames. We use the same unlabeled set with 5-million images as ResNet-based models. After transformation, we get around 90K videos. We train several popular algorithms with ResNet-50 backbone, and results are shown at the bottom of Table 3. Since augmentations in MoCo-v1 and MoCo-v2 are the same as VINCE, their performances are close to each other. With the stronger augmentation jigsaw, VINCE performs better on Faster RCNN.

Transformer-based Methods. In addition to pre-training with the traditional ResNet [23] backbone, we also provide the self-supervised result of transformer-based backbone on SODA10M dataset. We choose PVT-small [55] as the backbone by considering the training efficiency and easy deployment on object detection tasks. Experiment results in Table 4 show that simply applying traditional self-supervised learning methods results in a small drop (about 1-3%) in performance compared with ImageNet supervised pre-training. These results inspire us when pre-training a transformer-based model under a self-supervised scheme, we need to develop some specific algorithms based on its special structure, such as DeiT [52] and Swin-SSL [60].

Table 5: Detection results(%) of semi-supervised models on SODA10M dataset. Pseudo labeling (50K), Pseudo labeling (100K) and pseudo labeling (500K) means using 50K, 100K and 500K unlabeled images, respectively.

Model	mAP	AP50	AP75	Pedstrian	Cyclist	Car	Truck	Tram	Tricycle
Supervised	37.9	61.6	40.4	31.0	43.2	58.3	43.2	41.3	10.5
Pseudo Labeling (50K)	39.3 ^{+1.4}	61.9	42.4	32.6	44.3	60.4	43.8	42.4	12.1
Pseudo Labeling (100K)	39.9 ^{+2.0}	62.7	42.6	33.1	45.2	60.7	44.8	43.3	12.1
Pseudo Labeling (500K)	38.5 ^{+0.6}	61.0	41.3	32.1	43.4	59.6	42.6	42.2	11.0
STAC [47]	42.8 ^{+4.9}	64.8	46.0	35.7	46.4	63.4	47.5	44.4	19.6
Unbiased Teacher [39]	46.2 ^{+8.3}	70.1	50.2	33.8	50.2	67.9	53.9	55.2	16.4

4.4 Semi-Supervised Learning Benchmark

Semi-supervised learning has also attracted much attention because of its effectiveness in utilizing unlabeled data. We compare the naive pseudo labeling method with present state-of-the-art semi-supervised methods for object detection (*i.e.*, STAC [47] and Unbiased Teacher [39]) on 1-million unlabeled images considering the time limit. Both methods achieve high performance with only 1-million unlabeled images. For pseudo labeling, we first train a supervised model on the training set with the ResNet-50 [23] backbone for 12 epochs. Then we predict results on the unlabeled set, a bounding box with a predicted score larger than 0.5 is selected as a predicted label. All semi-supervised methods exceed the results of using only labeled data. As for pseudo labeling, adding an

Table 6: Detection results(%) in different domains on SODA10M dataset. IN indicates pre-trained on ImageNet, and SD means pre-trained on SODA10M unlabeled set. ‘-’ means no validation image in this domain.

Model	Overall mAP	City street (Car)			Highway (Car)			Country road (Car)		
		Clear	Overcast	Rainy	Clear	Overcast	Rainy	Clear	Overcast	Rainy
Daytime										
Supervised	43.1	70.0	64.9	56.6	68.3	65.9	65.9	69.4	63.5	-
MoCo-v1 [21] IN	44.2 ^{+1.1}	71.5	65.8	56.9	69.0	66.8	67.3	72.0	66.0	-
MoCo-v1 [21] SD	43.8 ^{+0.7}	71.3	66.0	55.8	69.4	67.4	68.0	72.8	65.5	-
STAC [47]	45.3 ^{+2.2}	74.2	69.6	58.0	71.7	70.3	70.7	75.2	69.8	-
Unbiased Teacher [39]	47.7 ^{+4.6}	73.0	68.1	55.3	69.1	62.0	71.3	72.6	70.0	-
Night										
Supervised	21.1	36.3	37.7	-	37.5	37.3	79.5	38.9	72.8	-
MoCo-v1 [21] IN	22.0 ^{+0.9}	39.5	43.4	-	41.7	41.5	80.6	42.5	73.2	-
MoCo-v1 [21] SD	22.7 ^{+1.6}	41.6	46.2	-	42.1	41.8	79.8	45.4	74.1	-
STAC [47]	28.2 ^{+7.1}	45.5	46.8	-	46.2	45.6	83.7	47.2	75.4	-
Unbiased Teacher [39]	39.7 ^{+18.6}	65.3	66.2	-	66.2	67.2	83.6	67.5	75.2	-

appropriate amount of unlabeled data (50K to 100K) brings a greater improvement, but continuing to add unlabeled data (100K to 500K) results in a 1.4% decrease due to the larger noise. We follow the default settings in STAC and Unbiased Teacher, and change the input size to comply with SODA10M. Shown in in Table 5, the STAC exceeds pseudo labeling by 2.9%, and Unbiased Teacher continues to improve by 3.4% due to the combination of Exponential Moving Average (EMA) and Focal loss [36].

4.5 Discussion

We directly compare the performance of state-of-the-art semi/self-supervised object detection methods with supervised Faster-RCNN in Table 6. In this table, we illustrate the overall mAP for daytime/night domain and car detection results of 18 fine-grained domains consisting of different periods, locations and weather conditions.

Observation can be made that there exists a huge gap between the domain of daytime and night. Since the supervised method is only trained on the data during the daytime, the gap between day and night is particularly obvious. By adding diverse unlabeled data into training, the self/semi-supervised methods show a more significant improvement in the night domain. Specifically for semi-supervised learning, Unbiased teacher [39] surpasses STAC [47] by a large margin in the night domain because it can address pseudo-labeling bias issues caused by class imbalance existing in ground-truth labels and the overfitting issue caused by the scarcity of labeled data. Besides, semi-supervised methods work much better than self-supervised methods either from the aspect of overall performance or the training time (2.8×8 GPU days vs. 8.4×8 GPU days for Unbiased teacher and MoCov1 respectively in Appendix B).

Inspired by the above results, we summarize some guidance dealing with SODA10M dataset. For self-supervised learning, different from ImageNet pre-training, simple methods (e.g., MoCov1 [21]) achieve better results than the dense contrastive methods (e.g., DenseCL [56]) on SODA10M unlabeled set. Concentrating on driving scenes, semi-supervised methods work much better than self-supervised methods when finetuning on SODA10M labeled set, even with a smaller set of unlabeled data (1-million vs. 5-million). Better performance will be achieved when combining self-supervised and semi-supervised methods. For both self and semi-supervised learning, model architecture design and efficient training will be promising topics on SODA10M for future research.

5 Conclusion

In this work, we present SODA10M, a large-scale 2D autonomous driving dataset that provides a small set of high-quality labeled data and a large amount of unlabeled data collected from various cities under diverse weather conditions, periods and location scenes. Comparing with the existing self-driving datasets, SODA10M is 10x larger than the largest dataset available Waymo and obtained in much more diversity. Furthermore, we build a benchmark for supervised, self-supervised and semi-supervised learning in autonomous driving and show that SODA10M can serve as a promising dataset for training and evaluating different self/semi-supervised learning methods. We hope that SODA10M can promote the exploration and standardized evaluation of advanced techniques for robust and real-world autonomous driving systems in the research community.

Appendix for SODA10M: Towards Large-Scale Object Detection Benchmark for Autonomous Driving

A SODA10M dataset

We publish the SODA10M dataset, benchmark, data format and annotation instructions at our website <https://soda-2d.github.io>. It is our priority to protect the privacy of third parties. We bear all responsibility in case of violation of rights, etc., and confirmation of the data license.

License, Terms of use, Terms of privacy. The SODA10M dataset is published under CC BY-NC-SA 4.0 license, which means everyone can use this dataset for non-commercial research purpose. Find more details in Appendix F.

Dataset documentation. <https://soda-2d.github.io/documentation.html> shows the dataset documentation and intended uses.

Data maintenance. <https://soda-2d.github.io/download.html> provides data download links for users (in Google Drive & Baidu YunPan). We will maintain the data for a long time and check the data accessibility in a regular basis. We also plan to extend the scale of unlabeled data to a 100-million level to help develop robust models.

Benchmark and code. The codebases used in our benchmark are open-source. More details of the reproduction code and experiment settings are illustrated in Appendix B.

Data format & Evaluation metrics. Annotation files in SODA10M are stored in standard COCO format, which can be easily accessible to most object detection codebases. We follow the popular COCO API [37] to utilize the Average Precision metric for evaluating detection performance.

Limitations. The major limitation of SODA10M is that some domains exist in the unlabeled set but not in labeled sets, which raises the problem that we can not verify the domain adaptation abilities in these domains. To overcome the limitation, we plan to provide more labeled data in these domains in the future.

B Implement Details

In order to make the experiment results reproducible, we further provide detailed experimental settings for each method in this paper. The basic differences compared with default setting is that class number is set to 6, syncBN is on and multi-scale training (in supervised and semi-supervised methods) is utilized with scale $1920 \times (864, 907.2, 950.4, 993.6, 1036.8, 1080)$. Without specifying, all self-supervised and semi-supervised methods adopt ResNet50 [23] backbone. Our models are trained on servers with 8 Nvidia V100 GPU(32GB) cards with Intel Xeon Platinum 8168 CPU(2.70GHz).

B.1 Open-Source Codebase

Table 7: The codebases used in our benchmark.

Codebase	link
Detectron2 [57]	https://github.com/facebookresearch/detectron2
PVT [55]	https://github.com/whai362/PVT
OpenSelfSup	https://github.com/open-mmlab/OpenSelfSup
VINCE [18]	https://github.com/danielgordon10/vince
STAC [47]	https://github.com/google-research/ssl_detection
Unbiased Teacher [39]	https://github.com/facebookresearch/unbiased-teacher

B.2 Supervised Methods

Table 8: Implement details for supervised learning benchmark on SODA10M with 8 Tesla V100.

Model	Train split	Default Setting	Difference	GPU hours
RetinaNet [36] 1x	train set	Detectron2	1. backbone no freeze. 2. turn on precise_bn.	0.78×8
Faster RCNN [45] 1x	train set	Detectron2	same as above	0.83×8
Cascaded RCNN [2] 1x	train set	Detectron2	same as above	0.92×8

B.3 Self-supervised Methods

For self-supervised methods, considering time limit, 5-million unlabeled images (split 0, 2, 4, 6, 8) of SODA10M are used, while we also make full use of the other 5-million subset in a sequential training manner (mentioned in †).

Table 9: Implement details for semi-supervised learning benchmark on SODA10M with 8 Tesla V100.

Model	Train split	Default Setting	Difference	GPU days
MoCov1 [21], MoCov2 [5], SimCLR [4], SwAV [3], DenseCL [56]	5-million unlabeled	OpenSelfSup	60 epochs	8.40×8
DetCo [58]	5-million unlabeled	OpenSelfSup	same as above	14.1×8
MoCov1 [21]†, MoCov2 [5]†, SimCLR [4]†	10-million unlabeled	OpenSelfSup	same as above	16.8×8
MoCov1 [21], MoCov2 [5], SimCLR [4], BYOL [19] on PVT	5-million unlabeled	OpenSelfSup	same as above	8.60×8
MoCov1 [21], MoCov2 [5], VINCE [18], VINCE+Jigsaw [18] on VIDEO	5-million unlabeled to 90k videos	VINCE	1. 800 epochs 2. VINCE augmentations	2.80×8

When finetuning on SODA10M labeled set and other datasets (Cityscape [7] & BDD100K [64]), the setting keeps consistent with the supervised methods and MoCo [21] respectively.

B.4 Semi-supervised Methods

For semi-supervised methods, considering the time limit, only 1-million unlabeled images (split 0) of SODA10M are used. Compared with self-supervised methods, semi-supervised methods are much more efficient.

Table 10: Implement details for semi-supervised learning benchmark on SODA10M with 8 Tesla V100.

Model	Train split	Default Setting	Difference	GPU days
Pseudo Labeling(50K)	50K unlabeled	Detectron2	1. backbone no freeze. 2. turn on precise_bn.	0.21×8
Pseudo Labeling(100K)	100K unlabeled	Detectron2	same as above	0.39×8
Pseudo Labeling(500K)	500K unlabeled	Detectron2	same as above	2.00×8
STAC [47]	1-million unlabeled	STAC	same as default	2.50×8
Unbiased Teacher [39]	1-million unlabeled	Unbiased Teacher	same as default	2.80×8

C More Experiments

Table 11 shows the performance of existing self-supervised methods evaluated on SODA10M labeled set with a longer schedule and instance segmentation result on Cityscape [7] dataset. We observe that dense contrastive methods (Detco, DenseCL) show excellent results when pre-trained on ImageNet [8], but relatively poor pre-trained on SODA10M unlabeled set. For semantic segmentation performance on Cityscapes with MoCov1, the model pre-trained on SODA10M even surpasses the one pre-trained in ImageNet by 1.6%, further verifying the generalization ability of pre-training on SODA10M.

Table 11: Detection results(%) of self-supervised models evaluated on SODA10M labeled dataset (with object detection task) and Cityscapes (C) dataset (with instance segmentation task).

Pre-train Dataset	Method	Faster-RCNN 2x			RetinaNet 2x			Mask-RCNN 1x	
		mAP	AP50	AP75	mAP	AP50	AP75	mAP-C	AP50-C
	random init	29.6	49.8	31.2	20.9	35.4	21.4	25.4	51.1
	super. IN	38.7	61.0	41.5	35.0	57.0	36.0	32.9	59.6
ImageNet [8]	MoCo-v1 [21]	39.3	60.9	42.5	35.9	57.4	37.3	32.3	59.3
	MoCo-v2 [5]	40.4	62.7	43.6	37.4	59.1	39.3	33.9	60.8
	SimCLR [4]	37.9	61.0	40.4	32.7	53.3	33.8	32.8	59.4
	SwAV [3]	38.2	61.9	40.9	32.6	53.4	33.8	33.9	62.4
	DetCo [58]	39.8	62.1	43.3	35.8	57.5	37.5	34.7	63.2
	DenseCL [56]	40.6	62.9	43.8	37.5	59.4	39.2	34.3	62.5
SODA10M	MoCo-v1 [21]	38.7	60.9	41.1	33.4	56.2	34.3	33.9	60.6
	MoCo-v2 [5]	39.1	60.8	42.6	33.6	56.2	34.8	33.7	61.0
	SimCLR [4]	36.7	59.6	39.1	31.6	53.8	32.3	30.2	57.0
	SwAV [3]	36.0	59.8	37.9	29.7	50.0	30.4	29.4	57.7
	DetCo [58]	37.2	58.9	39.8	31.2	53.5	31.3	32.5	59.8
	DenseCL [56]	38.9	61.0	41.9	33.2	55.4	33.7	33.1	60.7

D Domain Illustration

The distribution of each fine-grained domain in the validation set, testing set and unlabeled set is shown in the Table 12, Table 13 and Table 14.

Table 12: The number of images in each domain in validation set.

	Daytime			Night		
	City street	Highway	Country road	City street	Highway	Country road
Clear	383	961	63	137	167	312
Overcast	597	517	240	288	627	59
Rainy	177	406	0	0	66	0

Table 13: The number of images in each domain in testing set.

	Daytime			Night		
	City street	Highway	Country road	City street	Highway	Country road
Clear	490	2024	250	1591	498	146
Overcast	1216	1103	481	361	237	133
Rainy	917	520	24	9	0	0

Table 14: The number of images in each domain in unlabeled set.

	Daytime				Night				Dawn/Dusk			
	Clear	Overcast	Rainy	Snowy	Clear	Overcast	Rainy	Snowy	Clear	Overcast	Rainy	Snowy
City street	2247K	1483K	458K	140K	1274K	582K	157K	71K	325K	215K	62K	22K
Highway	506K	311K	114K	4K	186K	58K	24K	0.70K	37K	27K	9K	0.17K
Country road	499K	333K	69K	7K	170K	40K	12K	1K	38K	23K	5K	0.50K
Residential	146K	154K	29K	20K	61K	40K	7K	10K	9K	1K	2K	2K

More images in each domain are shown in Fig. 6.



Figure 6: More examples of challenging environments in our dataset.

E Acknowledgements

We thank our two data suppliers, named Testin² and Speechocean³ (collected from King-IM-055), for helping us collect and annotate SODA10M dataset.

²<http://www.testin.cn>

³<http://en.speechocean.com>

F Terms of Use and Licenses

Description. Huawei Technologies Co. Ltd (the ‘Organizers’ ,we", "us", and "our",) provides public access to and use of data that it collects and publishes. The data are organized in datasets (the “Datasets”) may be accessed at <https://sslad2021.github.io/index.html>. Any individual or entity (hereinafter You” or “Your”) with access to the Datasets free of charge subject to the terms of this agreement (hereinafter “Dataset Terms”). By using or downloading the Datasets, you are agreeing to comply with the Dataset Terms and any licensing terms referenced below. Use of any data derived from the Datasets, which may appear in any format such as tables and charts, is also subject to these Dataset Terms.

Licenses. Unless specifically labeled otherwise, these Datasets are provided to You under the terms of the Creative Commons Attribution-NonCommercial-ShareAlike 4.0 International Public License (“CC BY-NC-SA 4.0”), with the additional terms included herein. The CC BY-NC-SA 4.0 may be accessed at <https://creativecommons.org/licenses/by-nc-sa/4.0/legalcode>. When You download or use the Datasets from the Website or elsewhere, You are agreeing to comply with the terms of CC BY-NC-SA 4.0, and also agreeing to the Dataset Terms. Where these Dataset Terms conflict with the terms of CC BY-NC-SA 4.0, these Dataset Terms shall prevail. We reiterate once again that this dataset is used only for non-commercial purposes such as academic research, teaching, or scientific publications. We prohibits You from using the dataset or any derivative works for commercial purposes, such as selling data or using it for commercial gain.

Sharing. We prohibits You from distributing this dataset or modified versions. It is permissible to distribute derivative works in as far as they are abstract representations of this dataset (such as models trained on it or additional annotations that do not directly include any of our data).

Trademark. All logos and trademarks used on this website are the properties of us or other third parties as stated if applicable. No content provided on the website shall be deemed as granting approval or the right to use any trademark or logo aforesaid by implication, lack of objection, or other means without the prior written consent of us or any third party which may own the mark. No individual shall use the name, trademark, or logo of us by any means without the prior written consent of us.

Privacy. We will take reasonable care to remove or scrub personally identifiable information (PII) including, but not limited to, faces of people and license plates of vehicles. Furthermore, We prohibits You from using the Datasets in any manner to identify or invade the privacy of any person even when such use is otherwise legal. If You have any privacy concerns, including to remove your name or other PII from the Dataset, please contact us by sending an e-mail to xu.hang@huawei.com.

Warranties. The datasets and the website (including, without limitation, all content and modifications of original datasets posted on the website) are provided “as is” and “as available” and without warranty of any kind, express or implied, including, but not limited to, the implied warranties of title, non-infringement, merchantability and fitness for a particular purpose, and any warranties implied by any course of performance or usage of trade, all of which are expressly disclaimed. Without limiting the foregoing, motional does not warrant that: (a) the content or modifications to the dataset are timely, accurate, complete, reliable or correct in their posted forms at the website; (b) the website will be secure; (c) the website will be available at any particular time or location; (d) any defects or errors will be corrected; (e) the website, content or any modifications are free of viruses or other harmful components; or (f) the results of using the website will meet your requirements. Your use of the website, the datasets, and any content is solely at your own risk. Any entity or individual who suspects that the content on the website (including but not limited to the datasets posted on the website) infringes upon legal rights or interests shall notify our contact xu.hang@huawei.com in written form and provide the identity, ownership certification, associated link (url), and proof of infringement. We will remove the content related to the alleged infringement by law upon receiving the foregoing legal documents.

Limitation of liability. In no event shall motional and its affiliates, or their directors, employees, agents, partners, or suppliers, be liable under contract, tort, strict liability, negligence or any other legal theory with respect to the website, the datasets, or any content or user submissions (i) for any direct damages, or (ii) for any lost profits or special, indirect, incidental, punitive, or consequential damages of any kind whatsoever.

Applicable Law and Dispute Resolution. Access and all related activities on or through the website shall be governed by, construed, and interpreted in accordance with the laws of the People’s Republic of China. You agree that any dispute between the parties arising out of or in connection with this legal notice or your access and all related activities on or through this website shall be governed by a court with jurisdiction in Shenzhen, Guangdong Province of the People’s Republic of China.

References

- [1] H. Caesar, V. Bankiti, A. H. Lang, S. Vora, V. E. Liong, Q. Xu, A. Krishnan, Y. Pan, G. Baldan, and O. Beijbom. nusences: A multimodal dataset for autonomous driving. In *CVPR*, 2020.
- [2] Z. Cai and N. Vasconcelos. Cascade R-CNN: delving into high quality object detection. In *CVPR*, 2018.
- [3] M. Caron, I. Misra, J. Mairal, P. Goyal, P. Bojanowski, and A. Joulin. Unsupervised learning of visual features by contrasting cluster assignments. In *NeurIPS*, 2020.
- [4] T. Chen, S. Kornblith, M. Norouzi, and G. Hinton. A simple framework for contrastive learning of visual representations. In *ICLR*, 2020.
- [5] X. Chen, H. Fan, R. Girshick, and K. He. Improved baselines with momentum contrastive learning. *arXiv:2003.04297*, 2020.
- [6] E. Cole, X. Yang, K. Wilber, O. Mac Aodha, and S. Belongie. When does contrastive visual representation learning work? *arXiv:2105.05837*, 2021.
- [7] M. Cordts, M. Omran, S. Ramos, T. Rehfeld, M. Enzweiler, R. Benenson, U. Franke, S. Roth, and B. Schiele. The cityscapes dataset for semantic urban scene understanding. In *CVPR*, 2016.
- [8] J. Deng, W. Dong, R. Socher, L.-J. Li, K. Li, and L. Fei-Fei. Imagenet: A large-scale hierarchical image database. In *CVPR*, 2009.
- [9] C. Doersch, A. Gupta, and A. A. Efros. Unsupervised visual representation learning by context prediction. In *ICCV*, 2015.
- [10] P. Dollar, C. Wojek, B. Schiele, and P. Perona. Pedestrian detection: A benchmark. In *CVPR*, 2009.
- [11] A. Dosovitskiy, J. T. Springenberg, M. Riedmiller, and T. Brox. Discriminative unsupervised feature learning with convolutional neural networks. In *NeurIPS*, 2014.
- [12] G. J. et al. YOLOv5. <https://github.com/ultralytics/yolov5>, 2021.
- [13] J. Gao, J. Wang, S. Dai, L.-J. Li, and R. Nevatia. Note-rcnn: Noise tolerant ensemble rcnn for semi-supervised object detection. In *ICCV*, 2019.
- [14] A. Geiger, P. Lenz, C. Stiller, and R. Urtasun. Vision meets robotics: The KITTI dataset. *IJRR*, 2013.
- [15] A. Geiger, P. Lenz, and R. Urtasun. Are we ready for autonomous driving? The KITTI vision benchmark suite. In *CVPR*, 2012.
- [16] S. Gidaris, P. Singh, and N. Komodakis. Unsupervised representation learning by predicting image rotations. In *ICLR*, 2018.
- [17] I. Goodfellow, J. Pouget-Abadie, M. Mirza, B. Xu, D. Warde-Farley, S. Ozair, A. Courville, and Y. Bengio. Generative adversarial nets. In *NeurIPS*, 2014.
- [18] D. Gordon, K. Ehsani, D. Fox, and A. Farhadi. Watching the world go by: Representation learning from unlabeled videos. *arXiv:2003.07990*, 2020.
- [19] J.-B. Grill, F. Strub, F. Altché, C. Tallec, P. Richemond, E. Buchatskaya, C. Doersch, B. Avila Pires, Z. Guo, M. Gheshlaghi Azar, B. Piot, k. kavukcuoglu, R. Munos, and M. Valko. Bootstrap your own latent: a new approach to self-supervised learning. In *NeurIPS*, 2020.
- [20] H. Guo, Y. Mao, and R. Zhang. Mixup as locally linear out-of-manifold regularization. In *AAAI*, 2019.
- [21] K. He, H. Fan, Y. Wu, S. Xie, and R. Girshick. Momentum contrast for unsupervised visual representation learning. In *CVPR*, 2020.
- [22] K. He, X. Zhang, S. Ren, and J. Sun. Spatial pyramid pooling in deep convolutional networks for visual recognition. *TPAMI*, 2015.
- [23] K. He, X. Zhang, S. Ren, and J. Sun. Deep residual learning for image recognition. In *CVPR*, 2016.
- [24] G. E. Hinton, S. Osindero, and Y.-W. Teh. A fast learning algorithm for deep belief nets. *Neural Computation*, 2006.
- [25] G. E. Hinton and R. R. Salakhutdinov. Reducing the dimensionality of data with neural networks. *Science*, 2006.

- [26] J. Hoffman, S. Guadarrama, E. S. Tzeng, R. Hu, J. Donahue, R. Girshick, T. Darrell, and K. Saenko. Lsda: Large scale detection through adaptation. In *NeurIPS*, 2014.
- [27] D. Hu, Q. Lu, L. Hong, H. Hu, Y. Zhang, Z. Li, A. Shen, and J. Feng. How well self-supervised pre-training performs with streaming data? *arXiv:2104.12081*, 2021.
- [28] J. Jeong, S. Lee, J. Kim, and N. Kwak. Consistency-based semi-supervised learning for object detection. In *NeurIPS*, 2019.
- [29] C. Jiang, H. Xu, W. Zhang, X. Liang, and Z. Li. SP-NAS: serial-to-parallel backbone search for object detection. In *CVPR*, 2020.
- [30] D. Kim, D. Cho, and I. S. Kweon. Self-supervised video representation learning with space-time cubic puzzles. In *AAAI*, 2019.
- [31] C.-W. Kuo, C.-Y. Ma, J.-B. Huang, and Z. Kira. Featmatch: Feature-based augmentation for semi-supervised learning. In *ECCV*, 2020.
- [32] Q. V. Le, W. Y. Zou, S. Y. Yeung, and A. Y. Ng. Learning hierarchical invariant spatio-temporal features for action recognition with independent subspace analysis. In *CVPR*, 2011.
- [33] H. Lee, A. Battle, R. Raina, and A. Ng. Efficient sparse coding algorithms. In *NeurIPS*, 2007.
- [34] H.-Y. Lee, J.-B. Huang, M. Singh, and M.-H. Yang. Unsupervised representation learning by sorting sequences. In *ICCV*, 2017.
- [35] T.-Y. Lin, P. Dollár, R. Girshick, K. He, B. Hariharan, and S. Belongie. Feature pyramid networks for object detection. In *CVPR*, 2017.
- [36] T.-Y. Lin, P. Goyal, R. Girshick, K. He, and P. Dollár. Focal loss for dense object detection. In *ICCV*, 2017.
- [37] T.-Y. Lin, M. Maire, S. Belongie, J. Hays, P. Perona, D. Ramanan, P. Dollár, and C. L. Zitnick. Microsoft COCO: common objects in context. In *ECCV*, 2014.
- [38] W. Liu, D. Anguelov, D. Erhan, C. Szegedy, S. Reed, C.-Y. Fu, and A. C. Berg. SSD: Single shot multibox detector. In *ECCV*, 2016.
- [39] Y.-C. Liu, C.-Y. Ma, Z. He, C.-W. Kuo, K. Chen, P. Zhang, B. Wu, Z. Kira, and P. Vajda. Unbiased teacher for semi-supervised object detection. In *ICLR*, 2021.
- [40] Z. Liu, Y. Lin, Y. Cao, H. Hu, Y. Wei, Z. Zhang, S. Lin, and B. Guo. Swin transformer: Hierarchical vision transformer using shifted windows. *arXiv:2103.14030*, 2021.
- [41] T. Miyato, S. Maeda, M. Koyama, and S. Ishii. Virtual adversarial training: A regularization method for supervised and semi-supervised learning. *TPAMI*, 2019.
- [42] M. Noroozi and P. Favaro. Unsupervised learning of visual representations by solving jigsaw puzzles. In *ECCV*, 2016.
- [43] D. Pathak, P. Krahenbuhl, J. Donahue, T. Darrell, and A. A. Efros. Context encoders: Feature learning by inpainting. In *CVPR*, 2016.
- [44] S. Qiao, W. Shen, Z. Zhang, B. Wang, and A. Yuille. Deep co-training for semi-supervised image recognition. In *ECCV*, 2018.
- [45] S. Ren, K. He, R. Girshick, and J. Sun. Faster r-cnn: Towards real-time object detection with region proposal networks. In *NeurIPS*, 2015.
- [46] M. Sajjadi, M. Javanmardi, and T. Tasdizen. Regularization with stochastic transformations and perturbations for deep semi-supervised learning. In *NeurIPS*, 2016.
- [47] K. Sohn, Z. Zhang, C.-L. Li, H. Zhang, C.-Y. Lee, and T. Pfister. A simple semi-supervised learning framework for object detection. *arXiv:2005.04757*, 2020.
- [48] N. Srivastava, E. Mansimov, and R. Salakhudinov. Unsupervised learning of video representations using lstms. In *ICML*, volume 37.
- [49] P. Sun, H. Kretschmar, X. Dotiwalla, A. Chouard, V. Patnaik, P. Tsui, J. Guo, Y. Zhou, Y. Chai, B. Caine, V. Vasudevan, W. Han, J. Ngiam, H. Zhao, A. Timofeev, S. Ettinger, M. Krivokon, A. Gao, A. Joshi, Y. Zhang, J. Shlens, Z. Chen, and D. Anguelov. Scalability in perception for autonomous driving: Waymo open dataset. In *CVPR*, 2020.
- [50] Y. Tang, J. Wang, B. Gao, E. Dellandrea, R. Gaizauskas, and L. Chen. Large scale semi-supervised object detection using visual and semantic knowledge transfer. In *CVPR*, 2016.
- [51] Y. Tian, O. J. Henaff, and A. v. d. Oord. Divide and contrast: self-supervised learning from uncurated data. *arXiv:2105.08054*, 2021.
- [52] H. Touvron, M. Cord, M. Douze, F. Massa, A. Sablayrolles, and H. Jégou. Training data-efficient image transformers & distillation through attention. *arXiv:2012.12877*, 2020.

- [53] A. van den Oord, Y. Li, and O. Vinyals. Representation learning with contrastive predictive coding. *arXiv:1807.03748*, 2019.
- [54] C. Vondrick, H. Pirsaviash, and A. Torralba. Anticipating visual representations from unlabeled video. In *CVPR*, 2016.
- [55] W. Wang, E. Xie, X. Li, D.-P. Fan, K. Song, D. Liang, T. Lu, P. Luo, and L. Shao. Pyramid vision transformer: A versatile backbone for dense prediction without convolutions. *arXiv:2102.12122*, 2021.
- [56] X. Wang, R. Zhang, C. Shen, T. Kong, and L. Li. Dense contrastive learning for self-supervised visual pre-training. In *CVPR*, 2021.
- [57] Y. Wu, A. Kirillov, F. Massa, W.-Y. Lo, and R. Girshick. Detectron2. <https://github.com/facebookresearch/detectron2>, 2019.
- [58] E. Xie, J. Ding, W. Wang, X. Zhan, H. Xu, Z. Li, and P. Luo. DetCo: Unsupervised contrastive learning for object detection. *arXiv:2102.04803*, 2021.
- [59] Q. Xie, M.-T. Luong, E. Hovy, and Q. V. Le. Self-training with noisy student improves imagenet classification. In *CVPR*, 2020.
- [60] Z. Xie, Y. Lin, Z. Yao, Z. Zhang, Q. Dai, Y. Cao, and H. Hu. Self-supervised learning with swin transformers. *arXiv:2105.04553*, 2021.
- [61] I. Z. Yalniz, H. Jégou, K. Chen, M. Paluri, and D. Mahajan. Billion-scale semi-supervised learning for image classification. *arXiv:1905.00546*, 2019.
- [62] L. Yao, H. Xu, W. Zhang, X. Liang, and Z. Li. SM-NAS: structural-to-modular neural architecture search for object detection. In *AAAI*, 2020.
- [63] T. Yao, Y. Zhang, Z. Qiu, Y. Pan, and T. Mei. Seco: Exploring sequence supervision for unsupervised representation learning. In *AAAI*, 2021.
- [64] F. Yu, H. Chen, X. Wang, W. Xian, Y. Chen, F. Liu, V. Madhavan, and T. Darrell. BDD100K: A diverse driving dataset for heterogeneous multitask learning. In *CVPR*, 2020.
- [65] S. Yun, D. Han, S. J. Oh, S. Chun, J. Choe, and Y. Yoo. Cutmix: Regularization strategy to train strong classifiers with localizable features. In *ICCV*, 2019.
- [66] R. Zhang, P. Isola, and A. A. Efros. Colorful image colorization. In *ECCV*, 2016.
- [67] S. Zhang, R. Benenson, and B. Schiele. Citypersons: A diverse dataset for pedestrian detection. In *CVPR*, 2017.